The Major, N^2-Gua Adduct of the (+)-*anti*-Benzo[*a*]pyrene Diol Epoxide Is Capable of Inducing G→A and G→C, in Addition to G→T, Mutations†

Scott A. Jelinsky,‡ Tongming Liu,§ Nicholas E. Geacintov,§ and Edward L. Loechler*,‡

Department of Biology, Boston University, Boston, Massachusetts 02215, and Department of Chemistry, New York University, New York, New York 10003

Received June 8, 1995; Revised Manuscript Received August 4, 1995⊗

ABSTRACT: Mutations induced by the (+)-*anti*-diol epoxide of benzo[*a*]pyrene [(+)-*anti*-B[*a*]PDE] were collected in the *supF* gene of the *Escherichia coli* plasmid pUB3. pUB3 was reacted with (+)-*anti*-B[*a*]-PDE and then either (1) transformed immediately into *E. coli* or (2) heated at 80 °C for 10 min and then cooled prior to transformation—the latter to probe mechanism [Rodriguez & Loechler (1993) *Biochemistry 32,* 1759]. Qualitatively, heating did not affect the mutagenic pattern, except at the major base substitution hotspot in *supF*, G115, where principally G→T mutations were obtained prior to heating, while after heating, G→A and G→C mutations became statistically significantly more prevalent. Several studies have suggested that a heat-induced chemical transformation of a (+)-*anti*-B[*a*]PDE adduct at G115 (e.g., into an apurinic site) is not likely to explain the change in mutational pattern. The most likely model is that (+)-*anti*-B[*a*]P-N^2-Gua is initially trapped in a metastable conformation giving principally G→T mutations, while heating induces a change to a stable conformation(s) resulting in G→T, A, and C mutations. This suggests that adduct conformational complexity is at the root of adduct mutational complexity. To investigate this model, a plasmid (B[*a*]P-G115-pRE1) with (+)-*anti*-B[*a*]P-N^2-Gua in the G115 sequence context is constructed using adduct site-specific techniques. Following transformation of B[*a*]P-G115-pRE1 into *E. coli* (ES87) cells, targeted G115→T (59%), A (22%), and C (19%) mutations are isolated from (+)-*anti*-B[*a*]P-N^2-Gua, which approximates the ratio obtained at G115 with (+)-*anti*-B[*a*]PDE itself. (+)-*anti*-B[*a*]P-N^2-Gua principally induced G→T mutations in another sequence context [5′-TGC-3′; Mackay et al. (1992) *Carcinogenesis 13,* 1415]. Collectively, these findings demonstrate that (+)-*anti*-B[*a*]P-N^2-Gua is able to induce all three base substitution mutations and that DNA sequence context can influence the qualitative pattern of mutations from (+)-*anti*-B[*a*]P-N^2-Gua. Finally, it appears that (+)-*anti*-B[*a*]P-N^2-Gua at G115 may be able to induce semitargeted G116→A mutations as well, although this conclusion is more tentative.

The ubiquitous environmental contaminant benzo[*a*]pyrene (B[*a*]P)[1] is an example of a polycyclic aromatic hydrocarbon and is known to be mutagenic and carcinogenic (reviewed in Harvey, 1991). Inside cells, B[*a*]P can be metabolized to its (+)-*anti*-diol epoxide [(+)-*anti*-B[*a*]PDE], which is thought to be one important carcinogenic metabolite. The major DNA adduct results from trans addition at N^2-Gua [(+)-*anti*-B[*a*]P-N^2-Gua, where trans is implied; Cheng et al., 1989; Sayer et al., 1991]. B[*a*]P may react with DNA following activation by other pathways (e.g., Phillips et al., 1985; Marnett, 1987; Cavalieri et al., 1990; Devanesan et al., 1992).

We have been studying (+)-*anti*-B[*a*]PDE mutagenesis in *Escherichia coli* (Benasutti et al., 1988; Loechler, 1989, 1994, 1995; Loechler et al., 1990; Mackay et al., 1992; Rodriguez et al., 1992; Rodriguez & Loechler, 1993a,b, 1995; Drouin & Loechler, 1993, 1995), as well as the corresponding metabolite of dibenz[*a,j*]anthracene (Gill et al., 1993a,b). Implicit in our work is the hypothesis that a carcinogen's ability to induce mutations is at the root of its carcinogenic potential. The pattern of mutation(s) observed in various oncogenes and tumor suppressor genes (e.g., p53) seems to reflect the mutational pattern of the suspected carcinogens (Greenblatt et al., 1994), which tends to support this notion. However, this must be viewed as an open question, since

† This work was supported by grants from the NIH (ES03775) and the American Cancer Society (CN-54) to E.L.L. and by the Office of Health and Environmental Research, Department of Energy (DE-FG02-86ER60405), to N.E.G.

* Author to whom correspondence should be addressed.
‡ Boston University.
§ New York University.

⊗ Abstract published in *Advance ACS Abstracts,* October 1, 1995.

[1] Abbreviations: B[*a*]P, benzo[*a*]pyrene; (+)-*anti*-B[*a*]PDE, (+)-*r*-7,*t*-8-dihydroxy-*t*-9,10-epoxy-7,8,9,10,-tetrahydrobenzo[*a*]pyrene (*anti*); (+)-*anti*-B[*a*]P-N^2-Gua, the major adduct of (+)-*anti*-B[*a*]PDE (the trans addition adduct is implied unless stated otherwise); pRE0, pTZ19R with all three *Eae*I restriction sites removed and a −1 frameshift mutation in the *lacZ′* fragment; pRE1, pRE0 with O-G added into its *Hin*dII site; O-G, an unadducted decamer with the G115/G116 DNA sequence context (5′-GCGGCCAAAG-3′); O-G115, O-G decamer modified to contain (+)-*anti*-B[*a*]P-N^2-Gua in the G115 sequence context; O-G116, O-G decamer modified to contain (+)-*anti*-B[*a*]P-N^2-Gua in the G116 sequence context; B[*a*]P-G115-pRE1, pRE1 with (+)-*anti*-B[*a*]P-N^2-Gua in the G115 sequence context from *supF*; B[*a*]P-G116-pRE1, pRE1 with (+)-*anti*-B[*a*]P-N^2-Gua in the G116 sequence context from *supF*; G-pRE1, pRE1 constructed in parallel with B[*a*]P-G115-pRE1, and B[*a*]P-G116-pRE1, but with no adduct; AFB_1-*N*7-Gua, an adduct with aflatoxin B_1 bound at *N*7-Gua; MF, mutation frequency; the following terms, B/W^{R0}, WT^b, M^b, M^w, R0, B/W^{R4}, MF_{tot}, $MF_{G115\rightarrow T}$, and $Fr_{G115\rightarrow T}$, are defined in the last section of Materials and Methods; AP sites, apurinic/apyrimidinic sites; GHD, gapped heteroduplex DNA; Kf, DNA polymerase I Klenow fragment; X-Gal, 5-bromo-4-chloro-3-indolyl β-D-galactopyranoside; TE, 10 mM Tris-HCl (pH 8.0)/1 mM EDTA (pH 8.0); TAE, 40 mM Tris−acetate, 1 mM EDTA (pH 8.0).

0006-2960/95/0434-13545$09.00/0

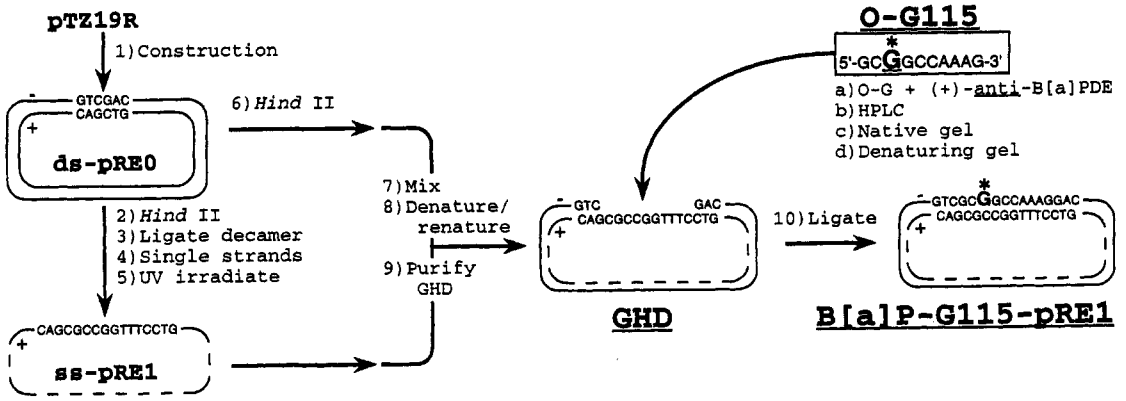

FIGURE 1: Strategy to situate a (+)-*anti*-B[*a*]P-N^2-Gua adduct in a sequence context corresponding to either G115 or G116 (see text). Steps a–d: O-G was reacted with (+)-*anti*-B[*a*]PDE and purified by HPLC, as well as native and denaturing gel electrophoresis. Step 1: pRE0 was constructed from pTZ19R by the removal of three *Eae*I restriction endonuclease sites. Steps 2 and 3: Construction of pRE1 by the introduction of a duplex oligonucleotide (5′-GCGGCCAAAG-3′/5′-CTTTGGCCGC-3′) into the unique *Hin*dII site in pRE0. Steps 4 and 5: ss-pRE1 was isolated and UV irradiated. Steps 6–9: ds-pRE0 was digested with *Hin*dII and mixed with UV irradiated ss-pRE1, and denatured/renatured to give gapped heteroduplex DNA (GHD), which was isolated and purified. Step 10: O-G115, which has a (+)-*anti*-B[*a*]P-N^2-Gua adduct in the G115 DNA sequence context (steps a–d), was covalently incorporated into the GHD via ligation.

carcinogen adduct levels are often very low, and a carcinogen may act indirectly, as demonstrated recently in one case (Cha et al., 1994).

(+)-*anti*-B[*a*]PDE induces a complex spectrum of mutations, including base substitutions (45%), frameshifts (24%), insertions (23%), and deletions (8%) (Rodriguez & Loechler, 1993a). Considering base substitution mutagenesis alone, which primarily involves mutation at G·C base pairs, a significant fraction of GC→TA (57%), GC→AT (23%), and GC→CG (20%) were all isolated (Rodriguez & Loechler, 1993a,b). This kind of mutational complexity is typical of bulky mutagens/carcinogens, but has not been explained.

In our work, an *E. coli* plasmid pUB3 was reacted with (+)-*anti*-B[*a*]PDE *in vitro*, which was subsequently transformed immediately into *E. coli* (ES87) cells (Rodriguez & Loechler, 1993a), and mutations in the *supF* gene of pUB3 were isolated and sequenced. In parallel, pUB3 adducted with (+)-*anti*-B[*a*]PDE was also heated at 80 °C for 10 min and then cooled to 0 °C prior to transformation (Rodriguez & Loechler, 1993b). We heated to probe mechanism, and the rationale for this has been described (Rodriguez & Loechler, 1993b; Drouin & Loechler, 1995). Quantitatively, heating caused an overall ~2-fold decrease in MF, which has been discussed (Rodriguez & Loechler, 1993b; Drouin & Loechler, 1995; Loechler, 1995). Qualitatively, the only statistically significant change in mutational pattern was observed at the major base substitution hotspot, G115, where prior to heating, G→T mutations (87%) dominated, while after heating G→T mutations (45%) were still prevalent, but there was a statistically significant increase in G→A (21%) and G→C (33%) mutations.

It is our belief that by understanding how heating could cause a change in the qualitative pattern of mutagenesis, we would be closer to understanding the mechanism(s) by which bulky adducts induce mutations. One model for the results at G115 is that a heat-labile adduct (e.g., B[*a*]P-*N*7-Gua) causes one pattern of mutagenesis prior to heating, while heating causes hydrolysis of the labile adduct, leaving an apurinic site (AP site), which results in a different mutational pattern. We have ruled out a significant role for AP sites at G115, as well as elsewhere (Drouin & Loechler, 1993). A second model is that heating causes a chemical modification of a (+)-*anti*-B[*a*]PDE adduct at G115 other than AP site formation. The only unstable adduct that we could detect was (+)-*anti*-B[*a*]P-N^2-Gua itself (Drouin & Loechler, 1995). However, this instability is not likely to account for the qualitative change in mutagenic pattern at G115, because the reaction both is too slow and gives (+)-*anti*-B[*a*]P-tetraols, which should leave guanine intact in DNA.

Our current working hypothesis for the results at G115, as well as elsewhere, is that a single adduct [i.e., (+)-*anti*-B[*a*]P-N^2-Gua in this case] can adopt multiple conformations in DNA with different mutagenic consequences and that factors such as DNA sequence context and heating can influence adduct conformation. To investigate this hypothesis, we have initiated an adduct site-specific study in a G115 sequence context, which appears to be a conformationally sensitive site. Herein we report on the construction of and mutations resulting from a plasmid containing (+)-*anti*-B[*a*]P-N^2-Gua in the G115 sequence context.

MATERIALS AND METHODS

The 7(*R*),8(*S*)-dihydroxy-9(*S*),10(*R*)-epoxy-7,8,9,10-tetrahydrobenzo[*a*]pyrene ((+)-*anti*-B[*a*]PDE) was purchased from the National Cancer Institute Chemical Carcinogen Reference Standard Repository (lot no. 92-356-91-19). A 3 mM (+)-*anti*-B[*a*]PDE stock solution in a 19:1 tetrahydrofuran/triethylamine solution was prepared. All (+)-*anti*-B[*a*]P-containing material was handled as described previously (Benasutti et al., 1988), including working under yellow lights with it.

[γ-^{32}P]dATP (sp act. 3000 Ci/mmol) was obtained from New England Nuclear (Boston, MA). Restriction endonucleases, DNA polymerase I Klenow large fragment (Kf), T4 polynucleotide kinase, T4 DNA ligase, and β-agarase were purchased from New England Biolabs (Beverly, MA), except as noted. *Hin*dII was obtained from Stratagene (La Jolla, CA). Manufacturer's recommended buffers were used except as noted. All materials not explicitly mentioned were of the manufacturer's highest grade purity.

Strains were as described elsewhere (Rodriguez & Loechler, 1992).

Synthesis and Purification of O-G115 and O-G116 (Figure 1, Steps a–d). The oligonucleotide 5′-GCG$_{115}$G$_{116}$CC-AAAG$_{122}$-3′ (O-G) was synthesized on a Milligen 7500

DNA synthesis device using phosphoramidite chemistry and purified by HPLC using conditions described previously (Benasutti et al., 1988). The (+)-*anti*-B[*a*]PDE-modified oligonucleotides O-G115, O-G116, and O-G122 were synthesized from O-G using the general approach described previously (Cosman et al., 1990; Mao et al., 1995). Approximately 80 A_{260} units of O-G were dissolved in 0.5 mL of 20 mM sodium phosphate solution containing 1.5% triethylamine (pH ~11). Aliquots of the (+)-*anti*-B[*a*]PDE were added 3 times until the final (+)-*anti*-B[*a*]PDE:O-G ratio was 2:1. After each addition, the reaction was stirred gently for 24 h at 24 °C in the dark. The solutions were extracted with water-saturated ether after each step in order to remove the corresponding B[*a*]P-tetraols; residual ether was removed by gently bubbling nitrogen through the solution.

The ether-extracted reaction mixtures were subjected to reverse phase HPLC analysis (Mao et al., 1995) using a Hypersil-ODS 5 μm 250 × 4.6 mm column (Keystone Scientific, Inc., Bellefonte, PA) and a Waters HPLC system (Millipore Corp., Milford, MA). Elution employed a 15−75% methanol elution gradient (in 20 mM sodium phosphate, pH 7.0) over 90 min with a flow rate of 3.0 mL/min (Figure 2a). The stereochemical nature of the adduct in each isolated oligonucleotide was established by digestion of an aliquot with snake venom phosphodiesterase (Pharmacia LKB Biotechnology, Piscataway, NJ) and bacterial alkaline phosphatase (Sigma, St. Louis, MI) to the mononucleoside level (Cosman et al., 1990; Geacintov et al., 1991).

HPLC-purified oligonucleotides were 5′-end, ^{32}P-radiolabeled and purified by native (i.e., nondenaturing) polyacrylamide (20%) gel electrophoresis (Figure 1, step c). The major band was located by autoradiography, and material from it was isolated in 1 M triethylamine bicarbonate (pH 7.6) as described previously (Ojwang et al., 1989). Each oligonucleotide was diluted 4-fold, desalted using C18 Sep-Pak cartridges (Waters), eluted in 60% methanol, evaporated to dryness using a Savant Speedvac, and stored at −20 °C. Each oligonucleotide was resuspended in 20 μL of H_2O and further purified by denaturing (7 M urea) polyacrylamide (20%) gel electrophoresis and isolated as described above (Figure 1, step d). Purity was established as >99% (see Results) following gel electrophoresis and visualization using a Molecular Dynamics Phosphoimager Model SF with the software ImageQuant (version 3.3).

Plasmid Constructions. The strategy in Figure 1 was developed to study mutagenesis by (+)-*anti*-B[*a*]P-N^2-Gua in the G115 (and G116) sequence context. For this strategy to work, the plasmid must contain only a single *Eae*I site with the adduct in it. To start (Figure 1, step 1), pRE0 (2726 bp), which contains no *Eae*I sites, was constructed from pTZ19R: two *Eae*I sites (positions 320 and 1457) were removed in a single step by site-directed mutagenesis using the method of Sayers and Eckstein (1989), while the third site (position 36), which was flanked by two *Tfi*I sites, was removed in an unessential 140 bp fragment by *Tfi*I digestion and religation. In addition, 4 bp were removed from the unique *Sph*I site of pRE0 in a blunt-ending reaction (Benasutti et al., 1988), which introduces a −1 frameshift mutation into the polylinker region, such that the *lacZ′* fragment is out of frame.

A second plasmid, pRE1, was constructed by inserting a duplex decamer (5′-GCGGCCAAAG-3′/3′-CGCCGGTTTC-5′), which contained the G115/G116 sequence context, into pRE0 (Figure 1, steps 2 and 3) using the method of Basu et al. (1987); the addition of 10 bp restores the reading frame in *lacZ′*.

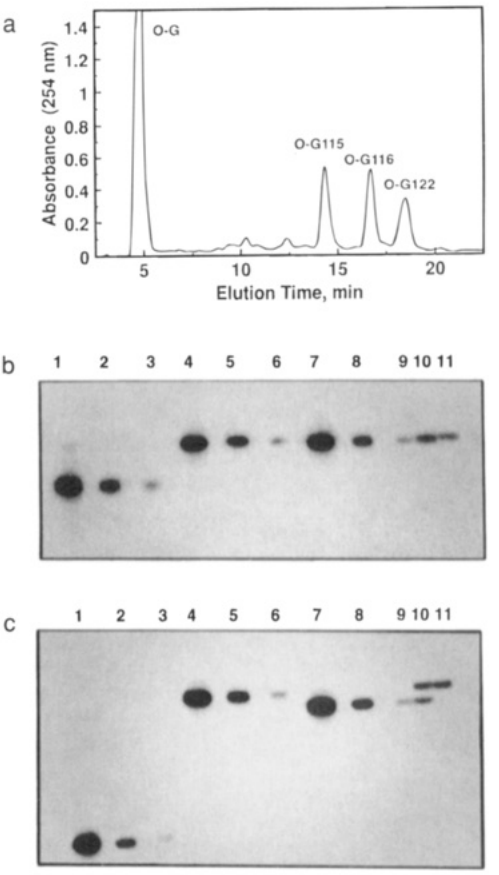

FIGURE 2: Purification and analysis of unadducted O-G, O-G115, which has (+)-*anti*-B[*a*]P-N^2-Gua in the G115 sequence context, and O-G116, which has (+)-*anti*-B[*a*]P-N^2-Gua in the G116 sequence context. Panel a: Following the reaction of (+)-*anti*-B[*a*]-PDE with O-G (5′-$G_{113}CG_{115}G_{116}CCAAAG_{122}$-3′), the products were separated by HPLC according to Mao et al. (1995). Peaks containing a single (+)-*anti*-B[*a*]P-N^2-Gua at G115 (O-G115), G116 (O-G116), and G122 (O-G122) as determined by a method based on the Maxam−Gilbert, G-specific DNA sequencing reaction (Mao et al., 1995) are indicated. Elution employed a 15−75% methanol elution gradient (in 20 mM sodium phosphate, pH 7.0) over 90 min with a flow rate of 3.0 mL/min. The material from O-G115 and O-G116, as well as O-G, was purified by both denaturing and native polyacrylamide gel electrophoresis, and then analyzed (panels b and c). Panel b (denaturing polyacrylamide gel electrophoresis) and panel c (native polyacrylamide gel electrophoresis): Lanes 1−3 show O-G in serial 10-fold dilutions. Similarly, lanes 4−6 show O-G115 and lanes 7−9 show O-G116 in serial 10-fold dilutions. Lane 10 shows a mixture of O-G115 and O-G116, while lane 11 shows O-G115 rerun.

Gapped Duplex Formation. ss-pRE1 (400 μg) was isolated from NM522 cells (Sambrook et al., 1989), irradiated with UV light (4800 J/m^2) in 2 mL of 10 mM Tris-HCl/1 mM EDTA (pH 8.0) (Benasutti et al., 1988), and ethanol precipitated and resuspended in TE (Figure 1, steps 4 and 5). (The rationale for step 5 is given in Results.) pRE0 (50 μg) was digested with *Hin*dII (100 units) to leave a blunt-end linear fragment (Figure 1, step 6), which was phenol/chloroform extracted, ethanol precipitated, and resuspended in TE (cf. 0.5 μg/μL).

Linear ds-pRE0 DNA (1 μg) was mixed with circular ss-pRE1 DNA (6 μg in 10 mM Tris-HCl/1 mM EDTA (pH

8.0), 100 mM NaCl) and heat denatured, and then slowly cooled to allow renaturation (Figure 1, steps 7 and 8; Benasutti et al., 1988). Material migrating as open circular DNA, which represents gapped heteroduplex pRE1 (GHD), was separated by 1.2% TAE−agarose (low melting point) gel electrophoresis and purified by a method involving a β-agarase digestion according to the manufacturer's (New England Biolab's) instructions (Figure 1, step 9). Purified GHD material was resuspended in 10 mM Tris-HCl/1 mM EDTA/20% glycerol (pH 8.0) and stored at −20 °C.

Construction of B[a]P-G115-pRE1, B[a]P-G116-pRE1, and G-pRE1 (Figure 1, Step 10). Approximately 167 ng (0.09 pmol) of GHD was mixed with either purified O-G, O-G115, or O-G116 [5.1 (1.6 pmol)−6.6 ng (2.0 pmol)]. Following ligation (400 units of T4 DNA ligase with 1 mM ATP for 18 h at 16 °C in 10 μL), the mixture was diluted to 50 μL and the products were purified by gel exclusion chromatography (Sepharose CL-4B, Pharmacia) equilibrated with 10 mM Tris-HCl, pH 8.0. The material in the void volume was collected and stored at +4 °C. The products are designated G-pRE1, B[*a*]P-G115-pRE1, and B[*a*]P-G116-pRE1, respectively.

Characterization of G-pRE1, B[a]P-G115-pRE1, and B[a]P-G116-pRE1. The presence of an adduct in a restriction site inhibits digestion by that corresponding restriction endonuclease, which has frequently been used to establish that an adduct is in an expected position (e.g., see Benasutti et al., 1988, and Gill et al., 1993a). G-pRE1, B[*a*]P-G115-pRE1, and B[*a*]P-G116-pRE1 (~10 ng) were each treated with *Eae*I (~6 units). Unadducted, unlabeled pRE1 (100 ng) was added to each digestion as an internal control to assess if *Eae*I digestion proceeded to completion as assessed by ethidium bromide staining (0.1 μg/mL) following agarose gel electrophoresis. The gels were subsequently dried and evaluated by phosphorimaging.

The presence of the adduct in the correct genome position was also assessed by a second method (rationale in Results). G-pRE1, B[*a*]P-G115-pRE1, and B[*a*]P-G116-pRE1 (~20 ng) were each treated with *Bam*HI and *Pst*I simultaneously. This mixture was denatured [i.e., treated as if it were a Sanger, dideoxy reaction (Rodriguez & Loechler, 1992)] and analyzed by phosphorimager following separation in a denaturing polyacrylamide (20%) gel.

Transformations. G-pRE1, B[*a*]P-G115-pRE1, and B[*a*]P-G116-pRE1 were transformed into ES87 or DH5α cells via electroporation (Rodriguez & Loechler, 1992). Competent cells (50 μL) were mixed with ~2 ng of plasmid and transformed by electroporation (Bio-Rad Gene Pulser; 2500 V, 100 Ω, 25 μF using a 0.2 cm gap). Recovery, growth, and plating were as described previously (Rodriguez & Loechler, 1992). In brief, following a 1 h recovery (37 °C in 1 mL of SOC media) after electroporation, a fraction of the transformation was plated on LB plates (with 100 μg/mL ampicillin and 12 μg/mL X-Gal) to determine the total number of transformants. The remainder of the cells were grown overnight in LB (60 mL; 100 μg/mL ampicillin). Plasmid DNA was isolated from these cells by a standard rapid plasmid preparation procedure (Rodriguez & Loechler, 1992) and designated R0 for "round zero" of mutant enrichment.

When appropriate, the SOS response was induced as described previously (Rodriguez & Loechler, 1992). In brief, ES87 cells were pelleted, resuspended in 10 mM $MgSO_4$, and irradiated with UV light (Ultraviolet Products, Inc., Model UAG-54) at 12.6 J/m^2, which was chosen to correspond to that used in our relevant random mutagenesis study (Rodriguez & Loechler, 1993b), and gave a cell survival of ~50%. Thereafter, the cells were harvested, washed, and resuspended in ice-cold 10% glycerol.

Mutations in the vicinity of the adduct would result in the elimination of the unique *Eae*I restriction site in pRE1. This serves as the basis for the mutant enrichment procedure, because digestion of R0 progeny would linearize wild type but not mutant plasmids, which, following transformation, would increase the fraction of progeny *Eae*I^r mutant plasmids because linearized wild type plasmids do not transform efficiently. Unfortunately, *Eae*I did not always digest wild type material to completion (see Results), so this enrichment procedure had to be repeated four times before mutants, which represented no more than ~2% of the progeny after R0, dominated the progeny plasmids. [By the ligase detection reaction (Barany, 1991), we were able to establish that the fraction of G→T, A, and C mutations at position G115 did not change in the course of this mutant enrichment procedure. The details of this procedure will be described elsewhere.] Following enrichment, plasmids were isolated from individual colonies and were sequenced by the Sanger dideoxy procedure (Rodriguez & Loechler, 1992).

Mutation Frequency (MF) Determination. MF at any particular site in the *Eae*I site of B[*a*]P-G115-pRE1, B[*a*]P-G116-pRE1, and G-pRE1 was calculated essentially as described previously for the same adduct in a *Pst*I site of a pUC19-based plasmid (Mackay et al., 1992). Briefly, the method is as follows. The *Eae*I site in pRE1 is in the *lacZ'* gene, which permits α-complementation to give β-galactosidase activity in appropriate cells, such as DH5α and ES87. β-Galactosidase activity can be monitored with the substrate X-Gal, which when cleaved gives colonies a blue color. Blue colonies have plasmids with *lacZ'* in-frame, which includes wild type as well as base substitution mutants in the *Eae*I site. Approximately 10% of the colonies were white and correspond in sequence to pRE0, which is a 10 bp deletion of pRE1, is one of the starting materials (Figure 1), and is also an *Eae*I^r mutant. The sources of progeny pRE0 have been discussed previously (Mackay et al., 1992).

$B/W^{R0} = [(WT^b + M^b)/(M^w)]$, where B/W^{R0} is the ratio (blue colonies/white colonies) before mutant enrichment (i.e., at R0), WT^b represent the number of blue wild type colonies, and M^b and M^w represents the number of blue and white mutant colonies, respectively. After four rounds of mutant enrichment (R4), wild type *Eae*I^s material has been virtually completely eliminated and the ratio (blue colonies/white colonies) corresponds to $B/W^{R4} = [(M^b)/(M^w)]$. Mutation frequency is calculated according to the following: $MF_{tot} = [(M^b)/(WT^b + M^b)] = [(B/W^{R4})/(B/W^{R0})]$. Individual blue colonies were isolated after R4 and sequenced. MF for any particular mutant (e.g., G115 → T) is simply as follows: $MF_{G115\rightarrow T} = (Fr_{G115\rightarrow T})(MF_{tot})$, where $Fr_{G115\rightarrow T}$ is the number of G115→T mutations isolated divided by the total number of mutants isolated.

RESULTS

Synthesis and Purification of Oligonucleotides Containing (+)-anti-B[a]P-N^2-Gua in the G115 and G116 Sequence Contexts (Figure 1, Steps a−d). O-G115, O-G116, and

O-G122, which have (+)-*anti*-B[*a*]P-N^2-Gua in the G115, G116, and G122 sequence context, respectively, were synthesized by reacting (+)-*anti*-B[*a*]PDE with the corresponding unadducted oligonucleotide O-G (5′-$G_{113}CG_{115}$-$G_{116}CCAAAG_{122}$-3′). (Adduction at G_{113} is inefficient.) Products were separated from one another by reverse phase HPLC (Figure 2a). Eluates at approximately 5, 14, 17, and 18.5 min are attributable to unadducted O-G and (+)-*anti*-B[*a*]PDE-modified oligonucleotides O-G115, O-G116, and O-G122, respectively. The sites of modification were established by modified Maxam−Gilbert sequencing techniques (Mao et al., 1995) as will be described in detail elsewhere (T. M. Liu et al., in preparation). The stereochemical characteristics of the modified Guas were established by HPLC analysis following digestion of O-G115, O-G116, and O-G122 to the mononucleoside level (Materials and Methods; Cosman et al., 1990; Geacintov et al., 1991). In each case (data not shown), a *trans*-(+)-*anti*-B[*a*]P-N^2-Gua mononucleoside adduct was obtained based upon coelution with an authentic standard as described by Cheng et al. (1989). CD spectra (data not shown) were also identical to the CD spectrum of the authentic *trans*-(+)-*anti*-B[*a*]PDE-N^2-Gua adducts (Cheng et al., 1989).

It was essential that O-G115 and O-G116 be >99% pure, especially from each other. Thus, the material isolated in Figure 2a was further purified by both native and denaturing polyacrylamide gel electrophoresis. We found that denaturing gel electrophoresis separates O-G115 and O-G116 from unidentified contaminants, but not from each other, while native gel electrophoresis separates O-G115 from O-G116, but not from these same unidentified contaminants.

Following these three steps of purification, the products were analyzed by denaturing polyacrylamide gel electrophoresis (Figure 2b). Lanes 4−6 show O-G115 in serial 10-fold dilutions; lane 4 has a single band with no contaminating bands at the level of <1%, as judged by comparison to the intensity of the band in lane 6, which is 100-fold less intense. Lanes 7−9 show similar results for O-G116; similarly, there are no contaminants at the level of <1%. Lane 11 shows O-G115 rerun, and lane 10 shows a mixture of O-G115 and O-G116; there is no significant separation. O-G is shown in lanes 1−3; there is a slight contaminant (~0.5% level) observable in lane 1.

Figure 2c shows results from native polyacrylamide gel electrophoresis, and lanes 1−11 correspond to lanes 1−11 in Figure 2b. By similar arguments, O-115 and O-G116 are >99% pure. Lane 10 shows that O-G115 and O-G116 separate from each other even when run in the same lane. [Lane 11 contains O-G115 (as in lane 6).] *In toto,* we conclude that both O-G115 and O-G116 are >99% pure and, importantly, do not significantly contaminate each other.

Construction of B[a]P-G115-pTZ. Figure 1 shows the strategy for our studies. One key feature is that an adduct at position G115 or G116 is embedded in an *Eae*I restriction site (5′-PyGGCCPu-3′), which must ultimately be a unique site in our construct. A plasmid pRE0 was constructed by removing three *Eae*I sites (leaving none) from pTZ19R, and introducing a −1 frameshift mutation into the polylinker region, such that the *lacZ′* fragment is out-of-frame (Figure 1, step 1). A second plasmid, pRE1, was constructed by inserting a duplex decamer, which contained the G115 sequence context, into pRE0 (Figure 1, steps 2 and 3); the addition of 10 bp restores the reading frame in *lacZ′*.

ss-pRE1, which had been UV irradiated for reasons explained below, was denatured/renatured (i.e., heteroduplexed) with pRE0, which was cleaved with *Hin*dII to give blunt-end, ds-linear DNA (Figure 1, steps 4−8). The product of interest--an open circular molecule with a 10-nucleotide gap [gapped heterodulpex DNA (GHD); Figure 1, step 9]—was purified by agarose gel electrophoresis. O-G, O-G115, and O-G116 were each ligated individually into this gapped duplex to give the products designated: G-pRE1, B[*a*]P-G115-pRE1, and B[*a*]P-G116-pRE1, respectively (Figure 1, step 10). Based on methods described previously (Benasutti et al., 1988), the efficiency of ligation was estimated to be ~72%, ~82%, and ~100%, respectively (data not shown).

Several points are worth noting. (1) The G115 sequence context in B[*a*]P-G115-pRE1 (Figure 1) is identical to that of G115 in the *supF* gene for two base pairs on the 5′-side and for 8 base pairs on the 3′-side (Rodriguez & Loechler, 1992). (2) The strategy in Figure 1 was devised such that (+)-*anti*-B[*a*]P-N^2-Gua in B[*a*]P-G115-pRE1 is in the nontranscribed strand of *lacZ′* and is replicated during lagging strand DNA synthesis, which corresponds to the situation in our random mutagenesis studies with (+)-*anti*-B[*a*]PDE, in which position G115 was in the nontranscribed strand of *supF* in pUB3 and was replicated during lagging strand DNA synthesis.[2] (3) In a situation where one DNA strand contains a lesion(s) from a bulky mutagen/carcinogen, while the complementary strand does not, progeny plasmids are preferentially derived from the strand containing no lesion(s), which is referred to as "strand bias" (Koffel-Schwartz et al., 1987). In order to minimize the generation of progeny plasmids from the strand not containing the B[*a*]P adduct, UV damage was introduced into it. (The UV damage is represented by the dashed line in Figure 1.) In the past, our experience has been that this method is helpful and nonproblematic (Mackay et al., 1992).

The products, G-pRE1, B[*a*]P-G115-pRE1, and B[*a*]P-G116-pRE1, were characterized. One means of establishing that a particular restriction site contains an adduct has been to show that the adduct blocks cleavage by the corresponding restriction endonuclease (*Eae*I in this case). B[*a*]P-G115-pRE1 and B[*a*]P-G116-pRE1 are both insensitive to cleavage by *Eae*I (Figure 3, lanes 4 and 6). Closed circular G-pRE1, which contains no adduct, is mostly cleaved by *Eae*I; however, digestion is not to completion since a large fraction of open circular material remains (Figure 3, lane 2). Several approaches to improve the efficiency of this digestion were taken, but none were successful.

The fact that G-pRE1 is not cleaved to completion by *Eae*I makes conclusions from the characterization reactions in

[2] In previous, random mutational studies with (+)-*anti*-B[*a*]PDE, G115/G116 is located in the *supF* gene of pUB3 (Rodriguez & Loechler, 1993a,b), while in the adduct site-specific studies described herein, G115/G116 is located in the polylinker region of *lacZ′*. pRE0 was chosen such that G115/G116 is in the nontranscribed strand of *lacZ′*, much as G115/G116 is in the nontranscribed strand in *supF* of pUB3. The relative orientation of transcription vs replication for *supF* in pUB3 is the same as *lacZ′* in pRE1. pRE1, which is derived from pTZ19R, has its single stranded DNA origin of replication oriented such that the oligonucleotide containing the adduct will ultimately end up in the strand that is replicated during lagging strand DNA synthesis. G115/G116 in *supF* were also replicated during lagging strand DNA synthesis of pUB3.

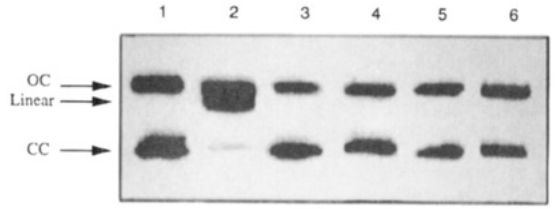

FIGURE 3: Characterization of G-pRE1, B[*a*]P-G115-pRE1, and B[*a*]P-G116-pRE1 by *Eae*I digestions. G-pRE1 was either not treated (lane 1) or treated (lane 2) with *Eae*I. B[*a*]P-G115-pRE1 was either not treated (lane 3) or treated (lane 4) with *Eae*I. B[*a*]P-G116-pRE1 was either not treated (lane 5) or treated (lane 6) with *Eae*I. Following agarose gel electrophoresis, the gel was dried and analyzed by phosphorimaging. The migrational positions of closed circular (cc), open circular (oc), and linear are indicated by the arrows.

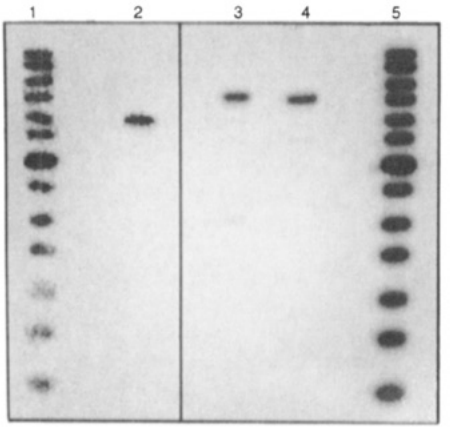

FIGURE 4: Characterization of G-pRE1, B[*a*]P-G115-pRE1, and B[*a*]P-G116-pRE1 following the liberation of an adduct-containing, 24-nucleotide fragment. G-pRE1 (lane 2), B[*a*]P-G115-pRE1 (lane 3), and B[*a*]P-G116-pRE1 (lane 4) were each digested with *Pst*I and *Bam*HI, which should liberate an adduct-containing, 24-nucleotide fragment of sequence: 5′-GGTCGCGGCCAAAG-GACTCTAGAG, where the underlining shows the sequence of the original oligonucleotide (i.e., O-G, O-G115, and O-G116) incorporated into the GHD. The samples were separated by denaturing polyacrylamide gel electrophoresis and analyzed by phosphorimaging. For size comparisons, lanes 1 and 5 show a ladder with bands at every 2 nucleotides between 8 and 32 nucleotides in length. Results in lanes 1 and 2 were from one experiment and from lanes 3−5 from a parallel experiment.

Figure 3 less firm. A second method was used to show that both B[*a*]P-G115-pRE1 and B[*a*]P-G116-pRE1 do indeed contain a lesion. Each sample was digested with *Pst*I and *Bam*HI, which should liberate an adduct-containing, 24-nucleotide fragment (sequence: 5′-GGTCGCGGCCAAAG-GACTCTAGAG-3′, where the underlining shows the sequence of O-G) following denaturation. Figure 4 shows that B[*a*]P-G115-pRE1 (lane 3) and B[*a*]P-G116-pRE1 (lane 4) both give one major band when analyzed by denaturing polyacrylamide gel electrophoresis. Material associated with these bands migrates more slowly than the corresponding major band from G-pRE1 (lane 2), presumably because the presence of the adducts retards migration, much as it did in the starting decamers (see Figure 2b,c).

B[*a*]P-G115-pRE1 (lane 3) and B[*a*]P-G116-pRE1 (lane 4) both have minor bands, which appear at positions ∼24, ∼22, and ∼16. Each band at position ∼24 is likely to represent a small amount (∼5%) of product with no adduct, since this band comigrates with the major band from G-pRE1 (lane 1). The bands at position ∼22 and ∼16 are likely to be attributable to ligation of a small fraction (∼5−10%) of the adducted oligonucleotide into the gapped duplex on the 3′- but not the 5′-side, and on the 5′- but not the 3′-side, respectively. (The fragments at ∼22 and ∼16 nucleotides correspond to a 20-mer and 14-mer, respectively, with an adduct that retards the migration by approximately 2 nucleotides each.) These kinds of incomplete ligation products have been observed in the past using similar construction strategies (Benasutti et al., 1988; Gill et al., 1993b).

We note that the fraction of B[*a*]P-G115-pRE1 that contains nicks on the immediate 5′- and 3′-sides is less than the total fraction of open circular (i.e., nicked) material as revealed in lane 3 of Figure 3. The latter is likely to be greater because of random nicks around the genome in some of B[*a*]P-G115-pRE1 (Benasutti et al., 1988; Gill et al., 1993b).

Mutants Derived from BP-G115-pRE1 and BP-G116-pRE1. BP-G115-pRE1 and BP-G116-pRE1, as well as unadducted G-pRE1, were transformed into both SOS-uninduced and SOS-induced ES87 cells. [ES87 was used because we wish to compare our results to our random adduction experiments with (+)-*anti*-B[*a*]PDE, in which we used ES87 cells (Rodriguez & Loechler, 1993 a,b).] Based on two transformations, the ratio of progeny yield from G-pRE1:BP-G115-pRE1:BP-G116-pRE1 was 1.0:0.51:0.53 (−SOS) and 1.0:0.33:0.34 (+SOS). [These values are difficult to interpret (see Discussion).]

Mutations at either position G115 or G116 eliminate the unique *Eae*I site in pRE1, rendering progeny plasmids resistant to cleavage by *Eae*I, which was used as the basis of the enrichment for mutations in the G115/G116 region (Materials and Methods). All single base substitution mutants isolated from G-pRE1, B[*a*]P-G115-pRE1, and B[*a*]P-G115-pRE1 (and corresponding MF) are presented in Table 1. Mutants with multiple base substitution mutations, which seemed to be randomly distributed throughout the *Eae*I site with no two being alike, as well as various deletions, were also isolated at a low frequency.[3] Because mutations of this type were also found in the corresponding unadducted samples at approximately the same frequency, they were unlikely to be attributable to the adduct and were ignored.

In a preliminary experiment, B[*a*]P-G115-pRE1 was also transformed into SOS-uninduced DH5α cells, and these results are also presented in Table 1. Finally, the construct with the adduct at G116 (i.e., B[*a*]P-G116-pRE1) was also transformed into SOS-induced ES87 cells. This work is incomplete, so we cannot report on it in detail; however, the results serve as a kind of control, so our preliminary results are reported: for mutations at position G116, G→T (4), G→A (2), and G→C (1) with total MF = 0.12% was obtained; for mutations at position G115, G→T (0), G→A (9), and G→C (4) with total MF = 0.22% was obtained.

[3] Multiple mutants were also obtained, and, with one exception (G-pRE1 sample), no two mutants were alike (compare to the wild type sequence: 5′-GCGGCCAAAG-3′). Several examples follow. B[*a*]P-G115-pRE1 (−SOS; 16 total): 5′-GCACCCAAAG-3′, 5′-GCGGGC-AACG-3′, 5′-ACGTCCGAAA-3′, 5′-GCTGGCAGAG-3′. B[*a*]P-G115-pRE1 (+SOS; 15 total): 5′-GCGGCGAATG-3′, 5′-GCGGCAGAAG-3′, 5′-GCATCGAAAG-3′, 5′-GCTACCGAAG-3′. G-pRE1 (−SOS; 4 total): 5′-GCCACCAAAG-3′, 5′-GCGGCCCGAG-3′, 5′-AGGGC-CTCTG-3′, 5′-GCATAAG-3′. G-pRE1 (+SOS; 8 total): 5′-GCGGA-CAAAG-3′, 5′-GCGGAGAAAG-3′, 5′-GAGGCCGCAG-3′, 5′-GC-CGAAG-3′.

Table 1: Single Base Substitution Mutations Isolated in the *EaeI* Site from the (+)-*anti*-B[*a*]P-N^2-Gua-Containing Plasmid B[*a*]P-G115-pRE1, and the Corresponding Control Plasmid G-pRE1, Which Contains No Adduct

	B[*a*]P-G115-pRE1												G-pRE1									
	ES87[a] cells (+SOS)[b]					ES87[a] cells (−SOS)[b]				DH5α[a] cells (−SOS)[b]				ES87[a] cells (+SOS)[b]					ES87[a] cells (−SOS)[b]			
N→[c]	T	A	C	G	tot[d]	MF[e]	T	A	C	G	tot[d]	MF[e]	T	A	C	G	tot[d]	MF[e]	T	A	C	G	tot[d]	MF[e]
C114[f]	ND[g]	3	—[h]	0	3	0.05	ND	1	—	1	2	0.03	ND	0	—	0	0	<0.01	ND	4	—	1	5	0.06	ND	2	—	2	4	0.02
G115	34	13	11	—	58	0.98	3	8	2	—	13	0.20	0	8	3	—	11	0.13	1	4	2	—	7	0.09	1	0	2	—	3	0.02
G116	1	13	1	—	15	0.25	3	8	1	—	12	0.19	1	10	4	—	15	0.18	0	0	1	—	1	0.01	0	0	1	—	1	0.01
C117	1	1	—	0	2	0.03	0	3	—	1	4	0.06	0	1	—	2	3	0.04	0	2	—	1	3	0.04	0	3	—	2	5	0.03
C118	0	3	—	2	5	0.08	0	0	—	4	4	0.06	0	1	—	1	2	0.02	0	7	—	1	8	0.10	0	2	—	0	2	0.01
A119	0	—	2	ND	2	0.03	0	—	1	ND	1	0.02	0	—	0	ND	0	<0.01	0	—	8	ND	8	0.10	0	—	1	ND	1	0.01

[a] Transformation was with either B[*a*]P-G115-pRE1 or G-pRE1 into either ES87 or DH5α cells (see text). [b] Cells were either SOS uninduced (−SOS) or induced (+SOS) (see text). [c] "N" indicates the base in the *EaeI* site scored for mutation and could be either A, C, or G, when represented by the base in the adduct-containing strand. [d] Total number of mutants (sum of the values in a row) isolated at any particular genome location. [e] MF is given in percent (e.g., 0.98 is 0.98% = 0.98×10^{-2}) at the indicated site and was calculated as described in Materials and Methods. [f] Base in the *EaeI* site of pRE1 numbered according to its corresponding base position in the *supF* gene. [g] "ND" means "not determinable", because the *EaeI* site, whose recognition sequence is 5′-PyGGCCPu-3′, is degenerate at two sites. [h] The dash corresponds to no mutation.

DISCUSSION

Mutations at G115 from (+)-anti-B[a]P-N^2-Gua at G115. For several reasons, we believe that the progeny from B[*a*]P-G115-pRE1 with mutations at G115 are from the (+)-*anti*-B[*a*]P-N^2-Gua adduct situated at position G115. (1) The oligonucleotide containing (+)-*anti*-B[*a*]P-N^2-Gua in the G115 sequence context was extensively purified, and there were no other detectable contaminants at the <1% level (Figure 2b,c). (2) MF at G115 from BP-G115-pRE1 is higher than MF for the control with no adduct (i.e., from G-pRE1) by ~10-fold (Table 1). In addition, the dominant mutation is G→T in the case of the former and G→A in the latter. (3) One alternative is that the mutations at G115 with B[*a*]P-G115-pRE1 are from the UV lesions in the strand that does not contain (+)-*anti*-B[*a*]P-N^2-Gua. This would require the (+)-*anti*-B[*a*]P-N^2-Gua adduct at G115 in the non-UV-lesion-containing strand in B[*a*]P-G115-pRE1 to enhance mutagenesis by the UV lesions compared to G-pRE1, which contains no adducts in the non-UV-lesion-containing strand. However, MF is lower from B[*a*]P-G116-pRE1 than from BP-G115-pRE1, which argues that the mere presence of an adduct in the non-UV-lesion-containing strand does not enhance mutagenesis sufficiently to make this explanation likely. (4) The results for (+)-*anti*-B[*a*]P-N^2-Gua in B[*a*]P-G115-pRE1 are both qualitatively and quantitatively consistent with the results for random mutagenesis with (+)-*anti*-B[*a*]PDE using pUB3. Qualitatively, (+)-*anti*-B[*a*]P-N^2-Gua gave a spectrum of mutations at G115 similar to (+)-*anti*-B[*a*]PDE itself, at least for the heated sample (discussed at greater length below). Quantitatively, SOS induction enhanced mutagenesis at G115 ~5-fold for (+)-*anti*-B[*a*]P-N^2-Gua (Table 1) and ~7-fold for (+)-*anti*-B[*a*]-PDE (Rodriguez & Loechler, 1993a) in the G115 sequence context. Furthermore, SOS induction enhanced G→T mutations more than G→A or G→C mutations both at G115 for (+)-*anti*-B[*a*]P-N^2-Gua (Table 1) and for (+)-*anti*-B[*a*]PDE when considering the whole data set (Rodriguez & Loechler, 1993a).

Comparison of Mutations at G115 from (+)-anti-B[a]PDE vs (+)-anti-B[a]P-N^2-Gua. G→T mutations (~59%) were most prevalent from (+)-*anti*-B[*a*]P-N^2-Gua in B[*a*]P-G115-pRE1, but G→A and G→C mutations (~41%) were also significant (Table 1). This pattern is reminiscent of the results at G115 for (+)-*anti*-B[*a*]PDE in random mutagenesis studies for the heated sample [G→T (45%), A (22%), and C (33%) (Rodriguez & Loechler, 1993b)]. We take this as circumstantial evidence that the mutations induced at G115 by (+)-*anti*-B[*a*]PDE are likely to be due to (+)-*anti*-B[*a*]P-N^2-Gua. However, the patterns are not identical (although this difference is not statistically significant), which may be real and important.

Our model for the role that heating has on the mutagenic pattern at G115 is that (+)-*anti*-B[*a*]P-N^2-Gua is trapped initially in a metastable conformation that gives rise to G→T mutations, but that heating allows the adduct to rearrange to its thermodynamically preferred conformation(s), from which it gives a significant fraction of G→T, A, and C mutations. [G115 may show this unique behavior because of its unique set of nearest neighbors (5′-C<u>G</u>G-3′) or because it is in a 5′-<u>G</u>GCC-3′ sequence, which is a context that has been shown to form an unusual bend in DNA (Goodsell et al., 1993).] Assuming that this model is correct, it was not a

surprise to us that the heated pattern of mutagenesis was obtained, given that BP-G115-pRE1 was manipulated extensively prior to transformation and (+)-*anti*-B[*a*]P-N^2-Gua would be expected to have arrived in its thermodynamically preferred state.

One of the future goals of this project is to identify conditions that might coax (+)-*anti*-B[*a*]P-N^2-Gua back to its putative metastable state at G115, which was detected in random mutagenesis with (+)-*anti*-B[*a*]PDE prior to heating and gave principally G→T mutations. If it could be shown that this adduct can reversibly change its mutagenic pattern, then this would add credence to the hypothesis that adduct conformational complexity is at the root of adduct mutational complexity.

Unfortunately, we could think of no convenient way to assess mutagenesis by (+)-*anti*-B[*a*]PDE itself in pRE1 to determine if G115 in pRE1 will behave like it did in pUB3 vis-a-vis the heating effect. However, the fact that both the G115 sequence context in pRE1 matches that in the *supF* gene of pUB3 over 11 base pairs and there are numerous correlations between the results for (+)-*anti*-B[*a*]PDE in pUB3 and (+)-*anti*-B[*a*]P-N^2-Gua in pRE1 are encouraging.

Our working hypothesis that mutational complexity arises from adduct conformational complexity leads to the question: do we believe that there is a simple one-to-one relationship between the three-dimensional structure of a lesion and the mutation it causes? (1) We believe that if an adduct is in a particular conformation when bypassed by a DNA polymerase, then it will always give rise to the same immediate biological effect (e.g., a premutagenic mispair). (2) Although seemingly straightforward, the previous statement is complicated for two reasons. (i) It is possible that the immediate biological effect can be reversed (e.g., by DNA polymerase proofreading). (ii) There are probably families of interrelated conformations that can be sampled by a DNA polymerase within a single encounter with an adduct. Because of this, the initial conformation of an adduct may potentially result in two different mutational responses, because after DNA polymerase encounters an adduct in a particular conformation, several different conformations may be sampled, and the biological effect may vary depending upon which conformation is ultimately bypassed. (Obviously, we believe that there may be exceptions, such as at G115.) (3) On the other hand, we believe that a single type of mutation may be induced by different conformations [e.g., G→T mutations: see Loechler (1994)].

The points raised in the previous paragraph are all conjecture. However, even if we could evaluate them in a general way, there may be considerable difficulty in assigning a particular mutation to a particular conformation, because the energy differences between any of the different putative mutagenic conformations (e.g., those associated with G→T vs G→A) is frequently small (i.e., <1 kcal/mol), given that the fraction of each mutation is frequently similar.

Mutation Frequency. MF reported in Table 1 is internally consistent, but cannot be interpreted as the inherent MF for (+)-*anti*-B[*a*]P-N^2-Gua in the G115 sequence context for several reasons.

(1) ES87 cells are wild type for all DNA repair pathways, notably UvrABC, which is known to repair B[*a*]P adducts; e.g., in another study, we found that ~80% of all (+)-*anti*-B[*a*]P-N^2-Gua adducts were repaired by the UvrABC system (Mackay et al., 1992). In this study, we have no data that speak to this issue.

(2) There may be non-B[*a*]P adduct-containing material and/or residual GHD contaminating B[*a*]P-G115-pRE1: the former from the fact that Figure 4 showed a small amount of G-pRE1 contaminating B[*a*]P-G115-pRE1, and the latter inferred from the fact that the ligation efficiency was not 100% (e.g., ~82% for B[*a*]P-G115-pRE1). We attempted to estimate a correction for MF based upon a procedure that had worked previously (Mackay et al., 1992) as follows. B-[*a*]P-G115-pRE1 (as well as B[*a*]P-G116-pRE1) was treated with Kf and dNTPs, which would fill-in GHD, and then with *Eae*I, which would cleave filled in GHDs as well as G-pRE1 contaminating B[*a*]P-G115-pRE1 (at least partially—see Figure 3) and, thereby, reduce their transformation efficiency (data not shown) compared to adduct containing B[*a*]P-G115-pRE1. We were never able to obtain consistent results from this experiment; however, in composite, the apparent MF increased ~2−3-fold following Kf/*Eae*I (data not shown), suggesting that MF in Table 1 for both B[*a*]P-G115-pRE1 and B[*a*]P-G116-pRE1 were low by approximately this amount. Another calculation, which is admittedly inexact, tends to support this estimate.[4] It is also difficult to interpret the relative progeny yield from G-RE1 vs B[*a*]P-G115-pRE1 and B[*a*]P-G115-pRE1 for the reasons discussed in this section.

Semitargeted Mutations at G116 from (+)-anti-B[a]P-N^2-Gua at G115. Several arguments support the notion that the mutations induced at G116 with B[*a*]P-G115-pRE1 (Table 1) may in fact be semitargeted mutations induced by (+)-*anti*-B[*a*]P-N^2-Gua at G115. (1) The oligonucleotide, O-G115, which was used to construct B[*a*]P-G115-pRE1, was shown to be contaminated with <1% of O-G116. Thus, it is extremely unlikely that the mutations at G116 from B[*a*]P-G115-pRE1 could be due to contamination from this species, especially since MF from B[*a*]P-G116-pRE1 itself is low (see last paragraph of the Results). (2) MF at G116 is >20-fold higher from B[*a*]P-G115-pRE1 than from the unadducted plasmid G-pRE1 in SOS-induced cells (Table 1). (3) Semitargeted mutations at G116 with B[*a*]P-G115-pRE1 were also observed independently in both SOS-uninduced ES87 and DH5α cells (Table 1). (4) (+)-*anti*-B[*a*]P-N^2-Gua at G116 appears also to induce semitargeted mutations at G115 (MF = 0.22%), in addition to targeted mutations at G116 (MF = 0.12%) (data not shown). These data are presented as an argument because MF is above the corresponding value for the unadducted plasmid, although the argument must be viewed as weak because MF is relatively low.

In spite of these arguments, there are several aspects of our data that make us cautious in concluding that (+)-*anti*-B[*a*]P-N^2-Gua at G115 can induce semitargeted mutations at G116. (1) In fact, MF at G116 is higher when (+)-*anti*-B[*a*]P-N^2-Gua is located at G115 (MF = 0.25%) than at G116 (MF = 0.12%). On the one hand, this serves as a

[4] Assuming the following: (1) G-pRE1 slightly contaminates B[*a*]P-G115-pRE1 (~7%, based on Figure 4); (2) gapped duplexes remain in B[*a*]P-G115-pRE1 (~18%, based on a ligation yield of 82%—see Results); (3) G-pRE1 and gapped duplexes transform with equal efficiency; and given that B[*a*]P-G115-pRE1 gave 52% (−SOS) or 33% (+SOS) as many progeny as G-pRE1 (see Results); it is possible to estimate that the true MF for the adduct in B[*a*]P-G115-pRE1 would be ~1.8−3.5-fold higher than that reported in Table 1.

kind of control, although this finding is unexpected. (2) The ratio of mutations induced at G115:G116 is 58:15 for (+)-*anti*-B[*a*]P-N^2-Gua (Table 1), but was 33:3 for (+)-*anti*-B[*a*]-PDE in random mutagenesis studies (Rodriguez & Loechler, 1993b). In addition, the mutations at G116 for (+)-*anti*-B[*a*]P-N^2-Gua were almost exclusively G→A (Table 1), while for (+)-*anti*-B[*a*]PDE there were two G→C and one G→A mutations (Rodriguez & Loechler, 1993b). It is difficult to know whether this difference is significant, because of the small number of mutants collected, and as noted above, the pathways of G→A and G→C mutations may be related.

In transformations with B[*a*]P-G115-pRE1, progeny plasmids were also isolated with mutations at position C_{114}, C_{117}, C_{118}, and A_{119} as well (Table 1). It is likely that these are background mutants, because they appear at a low frequency ($\leq$0.1%), which approximates their frequency of appearance in the control plasmid, G-pRE1.

Believable and convincing examples of semitargeted mutagenesis are just beginning to emerge. Fuchs has good evidence from an adduct site-specific study that a *C*8-Gua adduct of 2-(acetylamino)fluorene can induce semitargeted frameshift mutations in some DNA sequence contexts (Lambert et al., 1992). Essigmann and co-workers have preliminary evidence for substantial semitargeted mutagenesis occurring with AFB_1-*N*7-Gua (J. Essigmann, personal communication). Finally, there are examples in the literature where the mutagenic spectra of bulky mutagens/carcinogens show tandem base substitution mutations, where it has been argued that these events must result from coupled targeted and semitargeted events during the replication of a single adduct (Levy et al., 1992). In our own work with (+)-*anti*-B[*a*,*j*]ADE, the major mutations are G→A (~36%), but tandem GG→AA mutations comprise ~15% of the spectrum (Gill et al., 1993b). This implies a preference for semitargeted G→A mutations from (+)-*anti*-B[*a*,*j*]ADE; G116→A was the only semitargeted mutation from (+)-*anti*-B[*a*]P-N^2-Gua situated at G115 that was significantly above background. It will be of interest to determine if the preponderance of semitargeted G→A mutations implies something about mechanism.

ACKNOWLEDGMENT

We gratefully acknowledge the Cancer Research Program of the National Institutes of Health, Division of Cancer Cause and Prevention, Bethesda, MD, for providing (+)-*anti*-B[*a*]-PDE.

REFERENCES

Barany, F. (1991) *Proc. Natl. Acad. Sci. U.S.A. 88*, 189−193.
Basu, A. K., Niedernhofer, L. J., & Essigmann, J. M. (1987) *Biochemistry 26*, 5626−5635.
Benasutti, M., Ezzedine, Z. D., & Loecher, E. L. (1988) *Chem. Res. Toxicol. 1*, 160−168.
Cavalieri, E. L., Rogan, E. G., Devanesan, P. D., Cremonesi, P., Cerny, R. L., Gross, M. L., & Bodell, W. J. (1990) *Biochemistry 29*, 4820−4827.
Cha, R. S., Thilly, W. G., & Zarbl, H. (1994) *Proc. Natl. Acad. Sci. U.S.A. 91*, 3749.
Cheng, S. C., Hilton, B. D., Roman, J. M., & Dipple, A. (1989) *Chem. Res. Toxicol. 2*, 334−340.
Cosman, M., Ibanez, V., Geacintov, N. E., & Harvey, R. G. (1990) *Carcinogenesis 11*, 1667−1672.
Devanesan, P. D., RamaKrishna, N. V. S., Todorovic, R., Rogan, E. G., Cavalieri, E. L., Jeong, H., Jankowiak, R., & Small, G. J. (1992) *Chem. Res. Toxicol. 5*, 302−309.
Drouin, E. E., & Loechler, E. L. (1993) *Biochemistry 32*, 6555−6562.
Geacintov, N. E., Cosman, M., Mao, B., Alfano, A., Ibanez, V., & Harvey, R. G. (1991) *Carcinogenesis 12*, 2099−2108.
Gill, R. D., Rodriguez, H., Cortez, C., Harvey, R. G., Loechler, E. L., & DiGiovanni, J. (1993a) *Mol. Carcinog. 8*, 145−154.
Gill, R. D., Min, Z., Cortez, C., Harvey, R. G., Loechler, E. L., & DiGiovanni, J. (1993b) *Chem. Res. Toxicol. 6*, 681−689.
Goodsell, D. S., Kopka, M. L., Cascio, D., & Dickerson, R. E. (1993) *Proc. Natl. Acad. Sci. U.S.A. 90*, 2930−2934.
Greenblatt, M. S., Bennett, W. P., Hollstein, M., & Harris, C. C. (1994) *Cancer Res. 54*, 4855−4878.
Harvey, R. G. (1991) *Polycyclic aromatic hydrocarbons: Chemistry and cancer*, Cambridge University Press, Cambridge, U.K.
Koffel-Schwartz, N., Maenhaut-Michel G., & Fuchs, R. P. P. (1987) *J. Mol. Biol. 193*, 651−659.
Lambert, I. B., Napolitano, R. L., & Fuchs, R. P. P. (1992) *Proc. Natl. Acad. Sci. U.S.A. 89*, 1310−1314.
Levy, D. D., Groopman, J. D., Lim, S. E., Seidman, M. M., & Kraemer, K. H. (1992) *Cancer Res. 52*, 5668−5673.
Loechler, E. L. (1989) *Biopolymers 28*, 909−927.
Loechler, E. L. (1991) *Methods Enzymol. 203*, 458−476.
Loechler, E. L. (1994) in *The Toxicology of Aflatoxins: Human Health, Veterinary, and Agricultural Significance* (Eaton, D. L., & Groopman, J. D., Eds.) pp 149−178, Academic Press, Orlando, FL.
Loechler, E. L. (1995) *Mol. Carcinog. 13*, 213−219.
Loechler, E. L., Benasutti, M., Basu, A. K., Green, C. L., & Essigmann, J. M. (1990) in *Progress in Clinical and Biological Research, Vol. 340A, Mutation and the Environment, Part Al, Basic Mechanisms* (Mendelsohn, M. L., & Albertini, R. J., Eds.) pp 51−60, Wiley-Liss, New York.
Mackay, W., Benasutti, M., Drouin, E., & Loechler, E. L. (1992) *Carcinogenesis 13*, 1415−1425.
Mao, B., Xu, J., Li, B., Margulis, L. A., Smirnov, S., Ya, N. Q., Courtney, S., & Geacintov, N. E. (1995) *Carcinogenesis 16*, 357−365.
Marnett, L. J. (1987) *Carcinogenesis 8*, 1365−1373.
Ojwang, J. O., Grueneberg, D. A., & Loechler, E. L. (1989) *Cancer Res. 49*, 6529−6537.
Phillips, D. H., Hewer, A., & Grover, P. L. (1985) *Cancer Res. 45*, 4167−4174.
Rodriguez, H., & Loechler, E. L. (1993a) *Carcinogenesis 14*, 373−383.
Rodriguez, H., & Loechler, E. L. (1993b) *Biochemistry 32*, 1759−1769.
Rodriguez, H., & Loechler, E. L. (1995) *Mutat. Res. 326*, 29−37.
Rodriguez, H., Bhat, U. P., Snow, E. T., & Loechler, E. L. (1992) *Mutat. Res. 270*, 219−231.
Sambrook, J., Fritsch, E. F., & Maniatis, T. (1989) in *Molecular Cloning: A Laboratory Manual*, 2nd Ed., pp 4.32−4.48, Cold Spring Harbor Laboratory Press, Cold Spring Harbor, NY.
Sayer, J. M., Chadha, A., Agarwal, H. S. K., Yeh, H. J. C., Yagi, H., & Jerina, D. M. (1991) *J. Org. Chem. 56*, 20−29.
Sayers, J. R., & Eckstein, F. (1989) in *Protein Function* (Creighton, T. E., Ed.) pp 279−295, IRL Press, Oxford, England.

BI951283O